Journal of Polymer Research (2021) 28: 337
https://doi.org/10.1007/s10965-021-02694-9

ORIGINAL PAPER

Novel environmentally sustainable xylitol-based plasticizer: synthesis and application

B. Y. Hou[1,2] · L. Ren[1,2] · D. M. Fu[3] · Y. Y. Jiang[1,2] · M. Y. Zhang[1,2] · H. X. Zhang[1,2]

Received: 17 March 2021 / Accepted: 29 July 2021 / Published online: 11 August 2021

Abstract

Anhydroxylitol tripelargonate (AXP), a novel environmentally sustainable plasticizer for poly(lactic acid)/poly(butylene succinate) (PLA/PBS) blends, is successfully synthesized. The chemical structure of AXP is confirmed by FTIR and ^{1}H-NMR. The influence of varying the addition of AXP on mechanical property, thermal property, crystallization, rheological behavior and micromorphology of PLA/PBS blends is investigated in detail. The results are shown that the toughness and elongation at break of the blends are improved gradually with the increase of plasticizer addition, which indicates that plasticizer play a good plasticizing role in toughening blends. Furthermore, the introduction of AXP reduces the glass transition temperature (Tg) of the blends and simultaneously enhances its crystallization and processability. Observing the impact section of blends by SEM, it can be found that plasticizer AXP could change the blend from brittle fracture to ductile fracture. Additionally, the plasticization of AXP rivalled those petro-based plasticizers, and could be potential substitute to supplant O-benzene plasticizer in the future industry.

Keywords Xylitol · Poly(lactic acid) · Poly(butylene succinate) · Plasticizer · Crystallization

Introduction

In recent years, the overuse of non-degradable polymer materials has resulted in increasingly serious problems such as environmental pollution and "microplastics" [1, 2]. Polylactic acid (PLA), one of the excellent biodegradable materials, has attracted widespread attention in industrial applications due to its outstanding properties such as good biodegradability and biocompatibility [3, 4]. Nevertheless, PLA has some shortcomings comprising it is poor processability, rigid, brittle in nature and slow crystallization rate, which of these seriously limits the application of PLA [5–7].

✉ L. Ren
renl@ccut.edu.cn

✉ M. Y. Zhang
renl@ccut.edu.cn

[1] National Engineering Laboratory for Polymer Materials Synthesis and Application Technology, Changchun University of Technology, 130012 Changchun, China

[2] School of Chemical Engineering, Changchun University of Technology, Changchun 130012, China

[3] Department of Anesthesiology, Jilin Province Tumor Hospital, Changchun 130012, China

In order to improve the comprehensive performance of PLA, many researchers have studied ways to overcome the drawbacks of PLA such as blending with other polymers, copolymerization and adding plasticizers, etc. [8–13]. Several studies on PLA composites reported the use of biodegradable polymers or plasticizers to overcome their brittleness, with the advantage of controlling the blend properties by adjusting its composition [14–16]. Blending of PLA with poly(butylene succinate) (PBS) with flexible molecular chains has been proposed as a solution for the brittleness and poor processibility of PLA [17–20]. PBS act as flexibilizer in PLA and make the PLA chains easily movable, resulting in decreasing intermolecular forces. The PLA/PBS blend can not only overcome the brittleness of PLA, but also retain the biodegradability of the material. However, the PLA/PBS blend still has some limitations (such as poor toughness and low strength), many researchers have enhanced the properties of the blend by adding plasticizer. Plasticizers also decrease the glass transition temperature of polymeric materials, simultaneously overcoming their ductility. Pradeep et al. have investigated triphenyl phosphite (TPP) to plasticize the PLA/PBS blend, and experimental results are shown that the addition of TPP led to increase in the molecular weight of the polymer and the

melting temperature [21]. However, TPP has certain toxicity and cannot meet the environmental protection requirements. Pivsa-Art et al. have studied the effect of PEG on the properties of PLA/PBS blends [22]. The addition of PEG increased the elongation at break of the blend and reduced the Tg of the blend, but excessive addition of PEG would lead to phase separation of the blend, thereby performance degradation. Fortunati et al. are employed acetyl tributyl citrate (ATBC), isosorbide (ISE) and isocyanate-based plasticizers to plasticize the PLA/PBS blend [23]. ATBC and ISE are not good plasticizing effect for the blend and the isocyanate-based plasticizer has a good plasticizing effect, but raw materials are derived from non-renewable resources and certain toxicity, which did not conform to the requirements of green environmental protection.

In this study, a xylitol-based plasticizer (AXP) is prepared via using renewable resources xylitol and nonanoic acid as raw materials. By systematically changing the addition of AXP and PLA/PBS ratio, it could be feasible to tune the properties of blends. The effects of PLA/PBS ratio and AXP addition on the properties of the blends are investigated by means of mechanical property, thermal property, crystallization, rheological behavior and micromorphology.

Experiment

Materials

Xylitol, Nonanoic Acid and P-toluenesulfonic acid (PTS) used in this study are supplied by Shanghai Macklin Biochemical Co., Ltd. PLA (4032D) is a commercial product of Natureworks Co. Ltd., USA. PBS (1020MD) is purchased by Showa Denko.

Sample preparation

Synthesis of AXP

The AXP is synthesized via the two-step procedure, i.e. dehydration and esterification. The dehydration of xylitol (0.1 mol, 15.215 g), p-toluenesulfonic acid (0.00027 mol, 0.046 g) and toluene (100 ml) in the first step is performed under nitrogen atmosphere in a silicone oil bath at 110 ℃ to obtain anhydroxylitol. After 2 h, nonionic acid (0.33 mol, 52.219 g) and p-toluenesulfonic acid (0.00091 mol, 0.156 g) are further added into a 250 mL three-neck round bottom flask and magnetically stirred at 145 ℃. The reaction

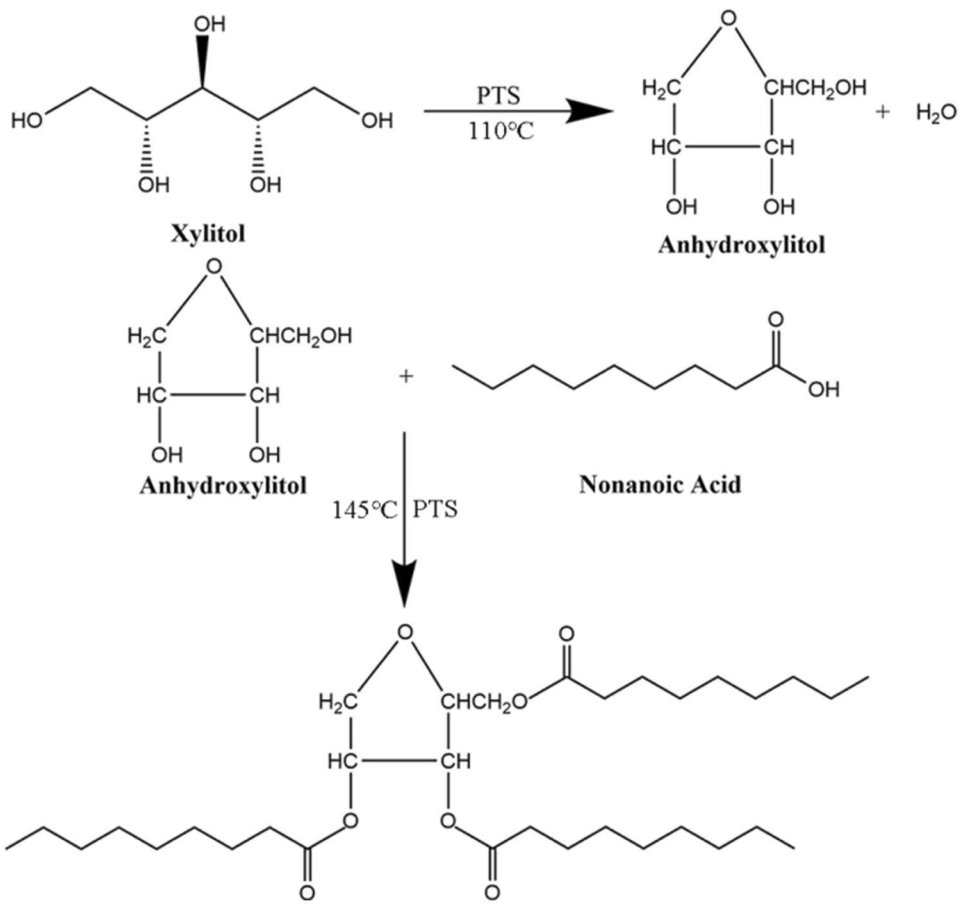

Scheme 1 Reaction equation of AXP

Table 1 The mixing compositions of PLA/PBS/AXP blends in this work

Sample	PLA (wt %)	PBS (wt %)	AXP (wt %)	Sample	PLA (wt %)	PBS (wt %)	AXP (wt %)
P15-0	100	0	15	**P0-20**	80	20	0
P15-5	95	5	15	**P5-20**	80	20	5
P15-10	90	10	15	**P10-20**	80	20	10
P15-15	85	15	15	**P15-20**	80	20	15
P15-20	80	20	15	**P20-20**	80	20	20
P15-25	75	25	15	**P25-20**	80	20	25
P15-30	70	30	15	**P30-20**	80	20	30
P15-40	60	40	15	**–**	–	–	–

mixture is continued for 3 h to obtain a pale-yellow oily product. The crude product is wished with saturated $NaCO_3$ solution, saturated NaCl solution and deionized water for three times respectively followed by evaporating at 65 ℃ for 3 h to obtain fine AXP.

The synthesis route and AXP display diagram are shown in Scheme 1.

Preparation of PLA/PBS/AXP blends

PLA/PBS/AXP blends are prepared by melt blending, and the reaction conditions: the temperature is 180 ℃, the rotating speed is 60 r/min, and the time is 6 min. The abbreviation and formulations of all the samples are listed in Tables 1 and 2. The preparation diagram of the blend is shown in Scheme 2.

Characterization

The chemical structures of AXP are confirmed by FTIR (Thermo Nicolet Avatar-360 spectrometer, America, KBr powder) over a range of 4000 -400 cm^{-1}.

AXP is analyzed by Bruker Avance III 400 Fourier transform nuclear magnetic resonance spectrometer (Bruker, Switzerland) operating at 400 MHz (^{1}H-NMR), and $CDCl_3$ is used as solvent.

The notched impact strength test is enforced on a cantilever beam impact testing machine (XJU22) at 23 ℃.

Table 2 Mechanical properties of the blends with different PLA/PBS ratios

Sample	Izod impact strength (J/m)	Elongation at break (%)	Modulus (MPa)
P15-0	35	208	1442
P15-5	80	119	1357
P15-10	152	142	1245
P15-15	218	167	1208
P15-20	251	198	1173
P15-25	153	250	1001
P15-30	87	334	971
P15-40	55	387	866

The tensile test is performed on an instron tensile tester system (Instron-3365, USA) with a crosshead speed of 20 mm/min at 23 ℃ by following the Chinese standard GB/T1040.1–2006. The samples are cut into dumbbell-shape with an effective size of 30 × 4 × 0.2 mm. Five samples are performed and took the average.

Dynamic mechanical analyses (DMA) of PLA/PBS/AXP blends are studied on a Diamond PE (Perkin-Elmer, USA), and the dimension of test samples is 30 mm × 10 mm × 1 mm. Specimens are subjected to a tension with amplitude of 20 μm and at a frequency of 1 Hz. The temperature range is set from 25 ℃ to 100 ℃ with a heating rate of 3 ℃/min. An experiment is always repeated by using another sample to make sure the reproducibility.

X-ray diffraction (XRD) is applied to investigate the crystal structures of the blends, which are performed on D/MAX 2000/PC instrument.

Rheological measurements are performed on a rheometer (AR2000EX, USA) at 150 ℃ and the angular frequency ranged from 0.1 to 100 rad/s.

Spherulite morphologies of the blends are observed by using LEICA DMRX polarized optical microscope (POM, Leica Microsystems, and Germany). The samples are heated from 25 to 190 ℃ with a rate of 10 ℃/min and then cooled to 110 ℃ for 2 h.

The thermal properties of the blends are recorded with a synchronous thermal analyzer (STA 6000, Perkin-Elmer, USA). The samples are heated from 25 to 190 ℃ and all samples are carried at a rate of 10 ℃/min.

Scanning electron microscopy (SEM) images are obtained by using a JSM6510 instrument (JEOL, Japan) with an accelerating voltage of 10 kV. All the samples with impact section are coated with a thin layer of gold on the fractured surface.

Results and discussion

AXP structure analysis

The FTIR spectra of xylitol, nonanoic acid and AXP are shown in Fig. 1. Compared with xylitol, AXP showed a strong and sharp band at around 1742 cm^{-1}, which

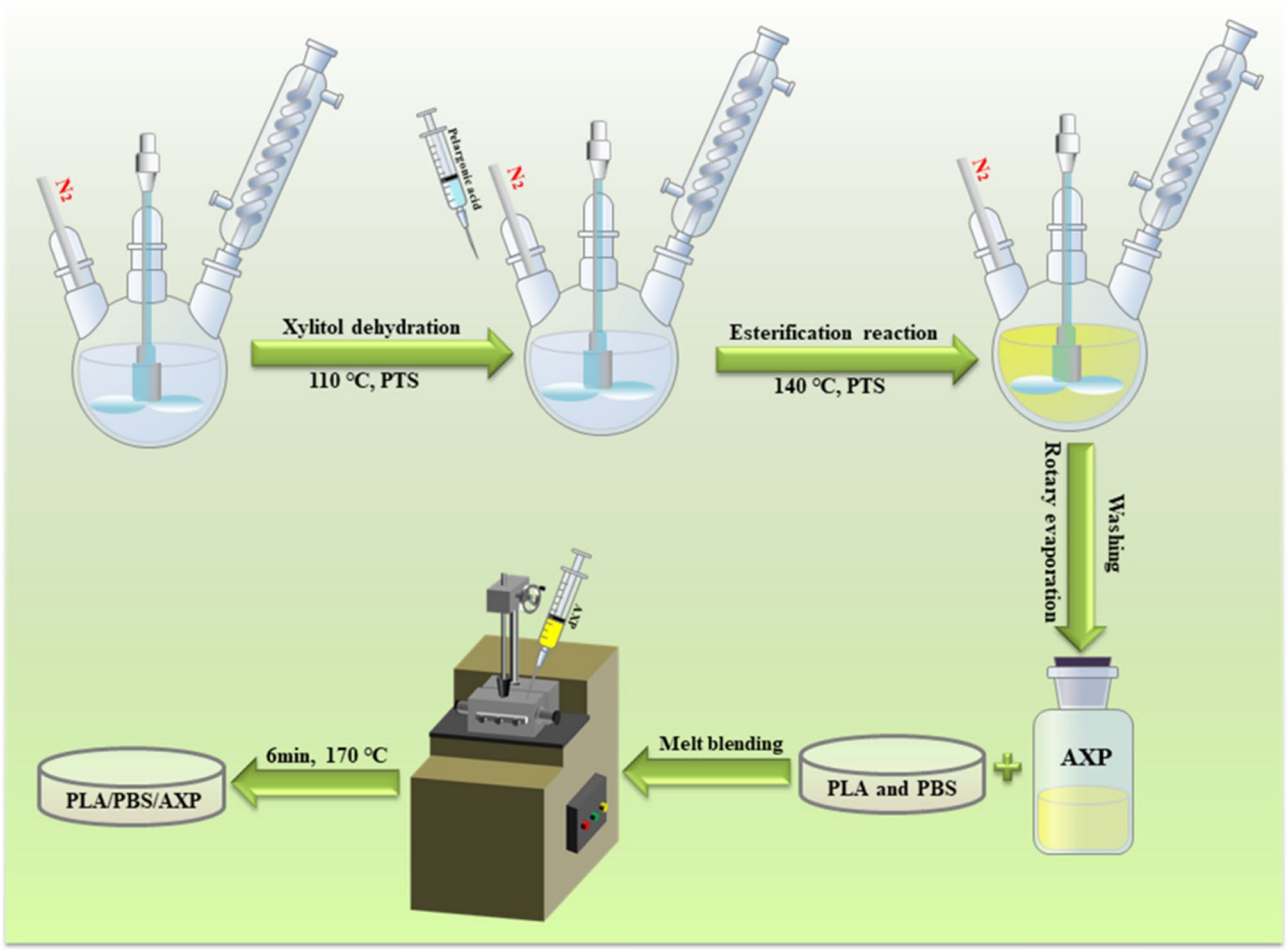

Scheme 2 Preparation flow chart of the blends

correspond to C = O. It is proved that xylitol successfully dehydrated. Meanwhile, the absorption peaks at around 1161 cm^{-1} and 1108 cm^{-1} of AXP could be assigned to the stretching vibration of C–O–C. Besides, the absorption peaks of AXP and xylitol at 2939 cm^{-1} and 2841 cm^{-1} are -CH_2- and -CH_3. The above data implied that the ester

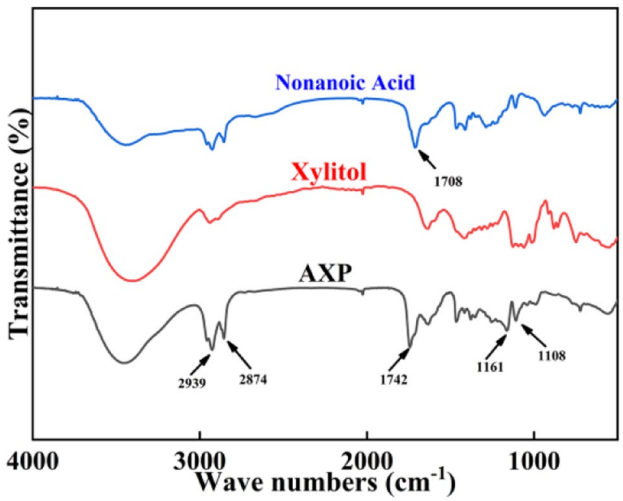

Fig. 1 FITR spectra of AXP and Xylitol samples

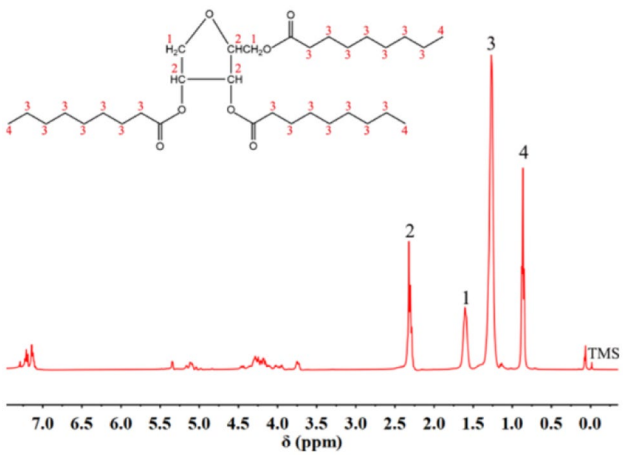

Fig. 2 ^{1}HNMR of spectra AXP plasticizer

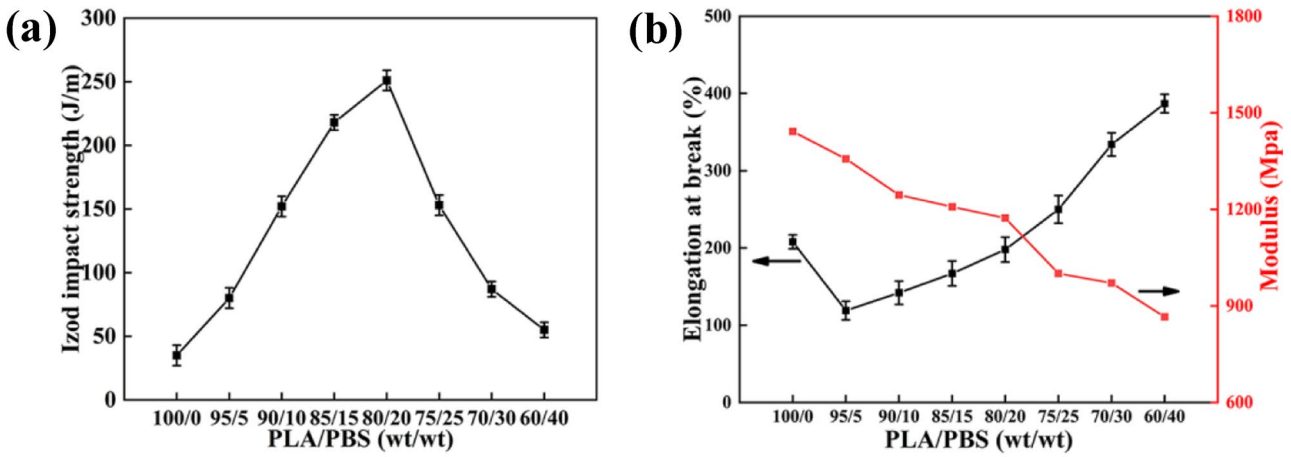

Fig. 3 Mechanical properties variation of the blends versus PLA/PBS ratio (**a**) Izod impact strength (**b**) Elongation at break and modulus

groups are formed and the esterification reactions are successful.

To further verify the chemical structures of AXP, ^{1}H-NMR spectra of AXP and xylitol are investigated, which is shown in Fig. 2. In Fig. 2, proton signals arising in the region of 0.8–2.4 ppm (H^1, H^2, H^3 and H^4) are attributed to the protons from AXP. Peaks appeared at 1.61 ppm (H^1) and 1.28 ppm (H^3) are assigned to -$(CH_2)_n$- and the proton signals at 2.32 ppm (H^2) and 0.87 ppm (H^4) represented -CH_3. The structure of AXP can be derived from the integrated intensity (I_H) of the proton absorption peak. With both ^{1}H-NMR and FTIR data, we could conclude that AXP are successfully prepared.

Matrix composition

S.H. Wu proposed that toughening polymer is closely related to polymer matrix and the PLA/PBS blend is used as the matrix in this work [24]. The influence of the different PLA/PBS ratio on the notch impact, elongation at break and tensile modulus properties of PLA/PBS/AXP blends (15 phr AXP) are shown in Fig. 3a and b. Clearly, it could be seized that the content of PBS as a flexibilizer in PLA vividly enhanced the toughness of PLA. For PLA/AXP blend (P15-0), the average value is 35 J/m, but the data increased dramatically to 251 J/m for the PLA/PBS/AXP blend (P15-20) containing 20wt% PBS. As expected,

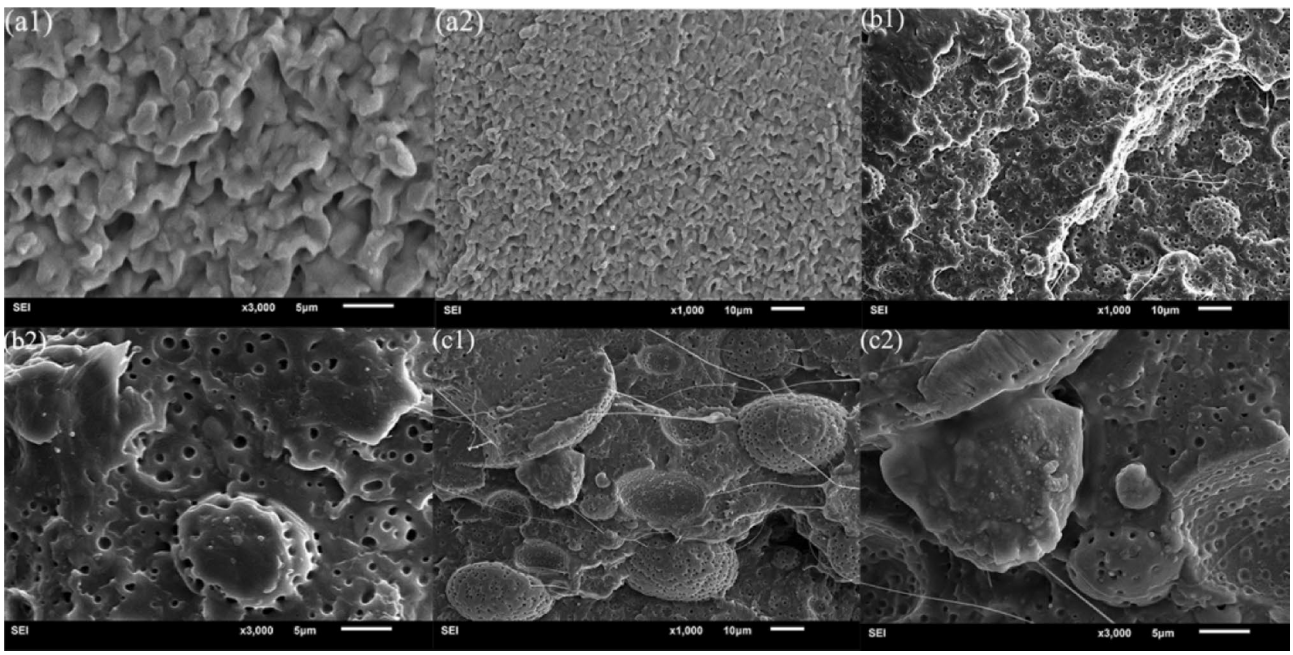

Fig. 4 SEM micrographs of fracture surface of blends with different PLA/PBS ratios from (**a**) P20-15, (**b**) P30-15, (**c**) P40-15

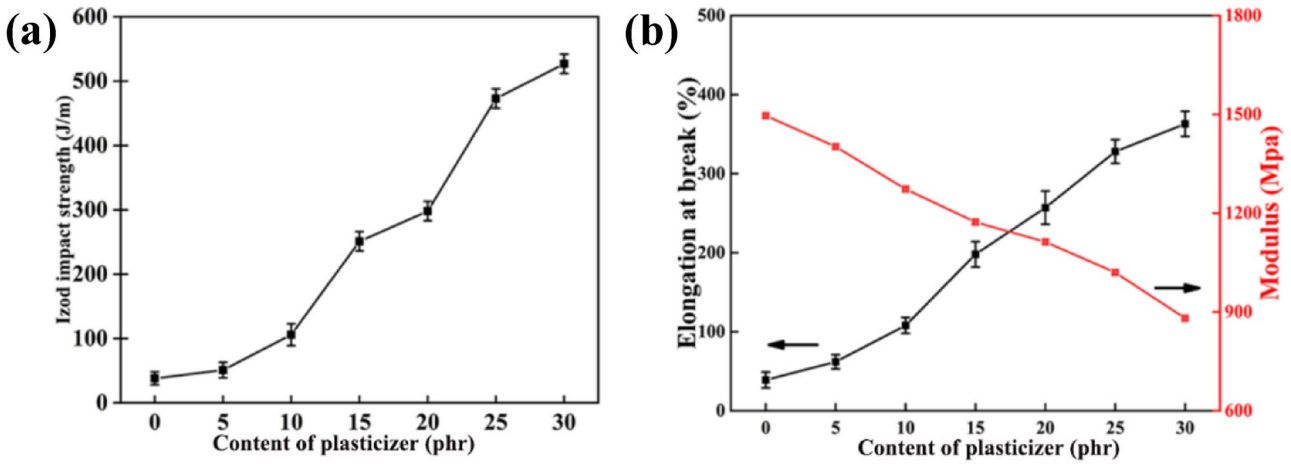

Fig. 5 Mechanical properties variation of the blends versus AXP contents (**a**) Izod impact strength (**b**) Tensile strength and modulus

the increase in toughness of PLA is observed when toughened with PBS due to the flexible molecular chain of flexibilizer created additional free volume of the molecular chain of blend, hence increasing ability to absorb impact energy. However, the decrease in impact strength is also observed when PBS addition greater than 20 wt% due to separation of PLA and PBS phases as seen from impact test results and the SEM micrographs (Fig. 4). It indicated that the blend is better toughness at 20 wt% PBS content, which is consistent with the experimental results of Bhatia A et al. [25].

In Fig. 3b, as the ratio of PLA/PBS increased, the tensile modulus of the blend showed a downward trend, and the elongation at break first decreased and then increased. When the ratio of PLA/PBS is 60/40, the tensile modulus decreased from 1442 to 886 MPa, and the elongation at break increased from 208 to 387%. It is due to PBS flexible molecular chains introduced in the blend, which is enhanced the ability to absorb energy when subjected to tensile stress, and easy to deformation under the same tensile stress.

The Fig. 4a showed the surface of the blend at 20 wt% PBS (P20-15). There are more "fibrils" on the surface and good compatibility, which proved that the 20wt% PBS and 80wt% PLA are not phase separation. In addition, the blend containing greater than 20wt% PBS content also showed PBS particles fall off on fractured surface and sizable voids are clearly observed in Fig. 4(b) and (c), which is presumably caused by the PBS phase separation in PLA matrix. Moreover, due to the increase in the PBS content, the particle size (i.e. mean diameter) increases. The same immiscible morphology trend was reported for blends of PLA with PBS Bhatia A et al. (2007) [25]. Hence, in order to obtain better toughness of the blend, the PLA/PBS ratio is 80/20 for research in the next work.

Mechanical properties

The mechanical properties of materials are the basic properties for evaluating the use value of materials [26]. In order to improve the toughness and ductility of materials, plasticizing materials is a very important method [6]. The plasticizing efficiency of AXP is further evaluated by impact strength test and tensile test. The notched impact strength, elongation at break and tensile modulus of curves of blends are shown in Fig. 5a and b and test results of these samples are

Table 3 Mechanical properties of the blends with different AXP contents

Sample	Izod impact strength (J/m)	Elongation at break (%)	Modulus(MPa)
P0-20	38	39	1496
P5-20	51	62	1402
P10-20	106	108	1273
P15-20	251	198	1173
P20-20	298	257	1113
P25-20	473	328	1020
P30-20	527	363	881

Table 4 Glass transition temperature (Tg) of the blends with different AXP contents

Sample	Glass transition temperature (℃)
P0-20	58.79
P5-20	51.49
P10-20	46.61
P15-20	44.49
P20-20	44.10
P25-20	43.18
P30-20	41.71

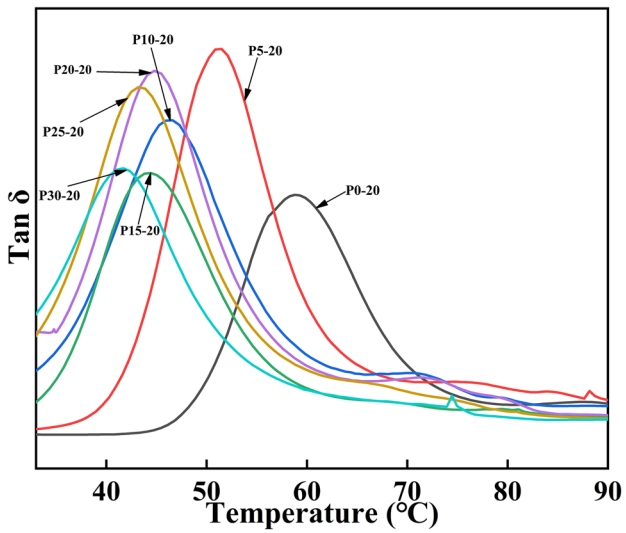

Fig. 6 DMA curves of the blends with different AXP contents

summarized in Table 3. As can be expected, the addition of AXP effective improved the toughness and elongation at break of blends, but poorer tensile modulus. When AXP addition is 30 phr (P30-20), the notched impact strength and elongation at break increased from 38 J/m and 39% to 527 J/m and 1286%, respectively. The tensile modulus decreased from 1496 to 881 Mpa. The improving elongation at break and the notch impact strength are due to the increase of the movement ability of the molecular chain after the addition of plasticizers. The interaction force between the molecular chains of the blend is reduce by these small molecules AXP via inserting the chains of blend. Besides, the enlargement in free volume vastly depressed the tensile modulus.

Glass transition temperature (T_g)

Glass transition temperature (T_g) is an effective index for the evaluation of plasticizing efficiency. DMA test is employed to investigate the variation of Tg in PLA/PBS/AXP blends. T_g values of PLA/PBS/AXP blends are shown in Table 4. It can be seen from the table that the T_g of the blend is revealed a downward trend with the increase of the AXP addition. When the amount of AXP is 30 phr (P30-20), the T_g is decreased from 58.79 ℃ to 41.71 ℃, which is 17.08 ℃ lower than the T_g of the blend without AXP (P20-0).

As a general rule, temperature consistent with loss tangent peak is taken as T_g, and the consequences are exhibited in Fig. 6. As shown in the figure, it is distinct that each sample has only one tanδ peak, indicating that the AXP is thermodynamically compatible with PLA/PBS matrix. It is also visible that T_g of PLA/PBS/AXP blends are lower than blends without AXP (P20-0). The addition of plasticizers moderated the intermolecular interactions of chains of blends, which the free volume of the blend enhanced. Therefore, AXP increased the mobility of chains of the blends. With the increase of the AXP addition, T_g of the corresponding blend decreased accordingly. Therefore, the plasticizing efficiency of AXP enhanced with the increase of the AXP addition.

Crystallization properties

Figure 7 showed POM photographs of the P0-20 and P30-20 blends crystallized at 110 ℃. With the addition of AXP, the spherulite size of the blend became larger and the number of spherulites would increase at the same time under the same conditions. is Because the small molecule AXP increased the free volume between the molecular chains of the blend, and raised the movement ability of the molecular chain, which is enhanced crystallization performance.

The effect of AXP on the crystal structures of PLA/PBS matrix is investigated. First, XRD is employed to determine the crystal structures of PLA, PBS and PLA/PBS/AXP blends, and the results are shown in Fig. 8. The pure PLA crystal has two characteristic diffraction peaks at 16.68

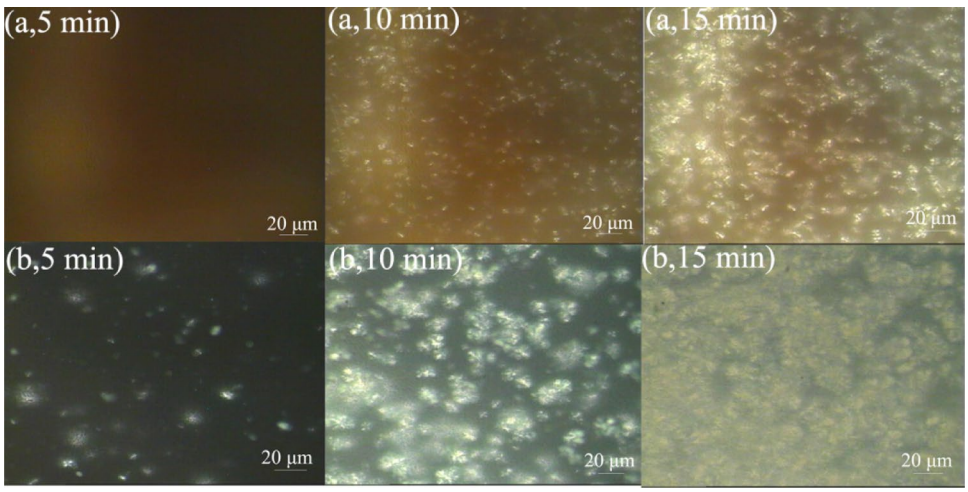

Fig. 7 POM image of the blends with different AXP contents (**a**) P0-20, (**b**) P30-20

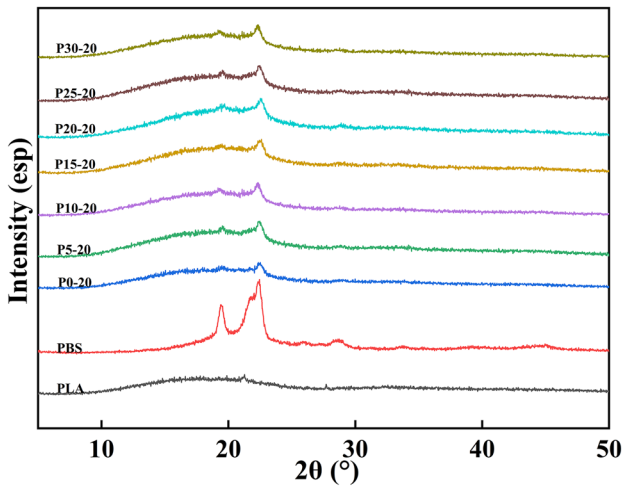

Fig. 8 XRD curves of the blends with different AXP contents

and 18.82. The pure PBS presented characteristic diffraction peaks at 19.65, 21.88, 22.81, which correspond to the (020), (021) and (110) crystallographic planes of PBS-phase [27]. The PLA/PBS blend (P20-0) showed characteristic diffraction peaks at 19.18 and 22.12, which indicated that the addition of PBS has changed the crystallization of PLA. PLA/PBS/AXP blends exhibited a similar XRD spectrum with PLA/PBS, which indicated that addition of AXP cannot induce the crystal form of PLA/PBS. As the addition of AXP increased, the area of the diffraction peak raised, which indicated that the introduction of AXP promoted the crystallization of the blend, and the crystal form of PLA/PBS matrix has not changed.

The cold-crystallization temperature (T_{cc}), the melting temperature (T_m) and the percentage of crystallinity (X_c) of PLA/PBS/AXP blends are shown in Table 5. The DSC curves obtained from the PLA/PBS/AXP blends are shown in Fig. 9. The cold crystallization is a phenomenon in which the polymer crystallizes well below the melting temperature (T_m) during the melting process. The PLA/PBS blend without AXP (P0-20) appeared not cold crystallization peak, but it appeared when AXP is added. With increasing AXP concentration, T_{cc} of blends decreased gradually and the cold crystallization enthalpy ($\triangle H_{cc}$) also gradually reduced. When the AXP addition is 30 phr (P30-20), T_{cc} decreased by 12.5 ℃. It is due to the presence of plasticizer, which facilitated the crystallize process of the PLA/PBS blend. The increasing molecular chain mobility enhanced the rate of crystallization of blend, which allowed the PLA/PBS blend to crystallize to a higher degree during cooling and enhanced cold crystallization capacity of the PLA/PBS blend. From the melting temperature point of view, the blend without AXP (P20-0) has two melting peaks, which of these are PBS melting temperature ($T_{m\text{-}PBS}$) is 122.5 ℃ and PLA melting temperature ($T_{m\text{-}PLA}$) is 161.3 ℃. With the increase of AXP addition, $T_{m\text{-}PBS}$ and $T_{m\text{-}PLA}$ decreased, and the melting enthalpy ($\triangle H_m$) also decreased. When the AXP addition is 30 phr, $T_{m\text{-}PLA}$ and $T_{m\text{-}PBS}$ reduced by 5.3 ℃ and 3.4 ℃, respectively. The addition of AXP enhanced the fluidity of the molecular chain, which led to an increase in the flexibility of the molecular chain of the blend, thereby reducing the melting point of the blend. When the AXP addition is 30 phr (P30-20), $T_{m\text{-}PLA}$ and $T_{m\text{-}PBS}$ reduced by 5.3 ℃ and 3.4 ℃, respectively. The addition of AXP enhanced the fluidity of the molecular chain, which is increased the flexibility of the molecular chain of the blend, and reduced the melting point of the blend.

The crystallinity of PLA in the blend ($X_{c,PLA}$) is calculated according to the following formula:

$$X_{c,PLA} = \frac{\Delta H_m - \Delta H_{cc}}{\Delta H_0 \times \omega_{PLA}} \times 100\% \quad (1)$$

Most commonly, an enthalpy of fusion of 93.6 $J \bullet g^{-1}$ and 200 $J \bullet g^{-1}$ is used for a 100% crystalline PLA and PBS, respectively [28, 29]. $\triangle H_m$ is the measured heat of fusion and $\triangle H_{cc}$ is the heat of cold crystallization. ω_{PLA} is the PLA content in the component.

Rheological behavior

Figure 10a showed the processing torque properties of blends at various addition of AXP. In Fig. 10a, as the addition of AXP increased, the processing torque of the blend gradually decreased. When the addition of AXP is

Table 5 DSC results of the blends with different AXP contents

Sample	T_{cc} (℃)	$T_{m\text{-}PBS}$ (℃)	$T_{m\text{-}PLA}$ (℃)	$\triangle H_{cc}$ ($J \bullet g^{-1}$)	$\triangle H_m$ ($J \bullet g^{-1}$)	$X_{c,PLA}$ (%)
PLA	–	–	168.0	–	18.08	19.32
PBS	–	124.7	–	–	62.21	-
P0-20	–	122.5	161.3	–	31.53	42.11
P5-20	104.9	121.8	159.4	8.04	29.50	28.66
P10-20	98.9	121.3	158.6	6.95	26.25	25.77
P15-20	96.7	120.5	157.9	6.01	23.32	23.12
P20-20	94.3	119.7	157.1	5.37	20.36	20.02
P25-20	92.7	119.3	156.4	4.40	18.20	18.43
P30-20	92.4	119.1	156.0	3.90	16.75	17.16

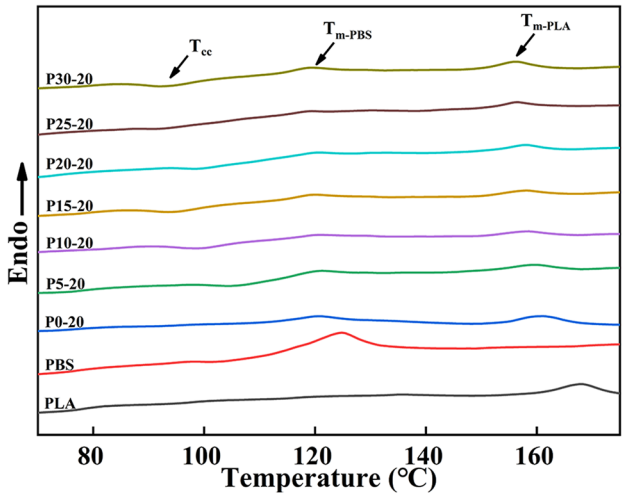

Fig. 9 DSC curves of the blends with different AXP contents

30 phr, the torque of the blend is 0.1 Nm at 6 min, which is 98.27% lower than that when no plasticizer is added. The introduction of AXP improved the processability of the blend. To thoroughly comprehend and the processability of plasticized PLA/PBS/AXP blends, a detailed research of the rheological behavior of these blends with varying AXP addition is inevitable. Figure 10b, c and d presented the complex viscosity properties (η*), the storage modulus properties (G') and the storage modulus (G") properties of blends on frequency at various addition of AXP at 150 ℃. In Fig. 10b, the complex viscosity exhibited a pronounced downtrend with the addition of AXP increased. For example, when ω is 10 rad/s and the addition of AXP is 15 phr, the η* of the blend is 43.6 Pa·s, which is nearly 77.6% lower than PLA/PBS blend (P0-20). Because AXP can weaken the interaction force between the molecular chains, and the η* of the blend is reduced. The corresponding G' and G" for these blends are shown in Fig. 10c and d, respectively. The storage modulus G' represents the energy stored by the material due to elastic deformation during the deformation process [30]. The loss modulus G" is the ability of the blend to transform energy into heat when deformed [31]. As expected, G' and G" of the blend decreased with increasing the addition of AXP at all frequencies. PLA/PBS and PLA/PBS/AXP (0–30 phr of AXP) exhibited the rheological behavior of a typical polymer melt as characterized by the G' smaller than the G". Both the G' and G" decreased with increasing AXP addition, it is due to AXP enhanced the movement ability of the molecular chain, and the molecular chain is also easy to slip when subjected to thermal shear, which resulted in improving processability of blends Furthermore, the addition of AXP decreased the intermolecular force and enhanced the mobility of the polymeric chains, which is improved the extensibility and the flexibility of the blend.

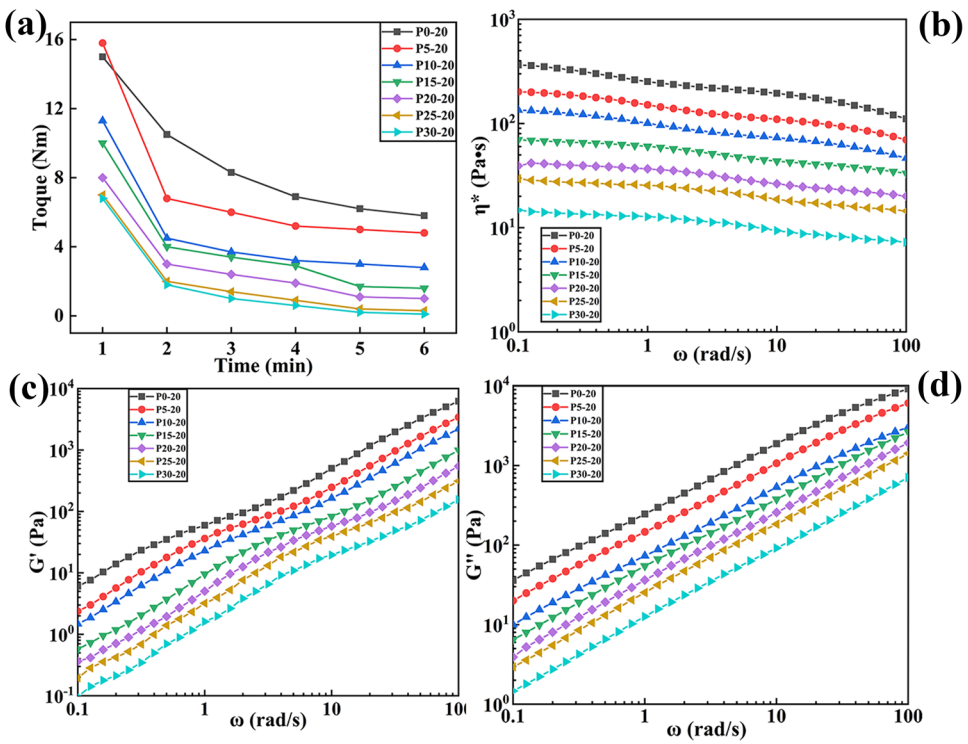

Fig. 10 The processability of the blends with different AXP contents (**a**) Processing torque (**b**) Complex viscosity (**c**) Storage modulus (**d**) Loss modulus

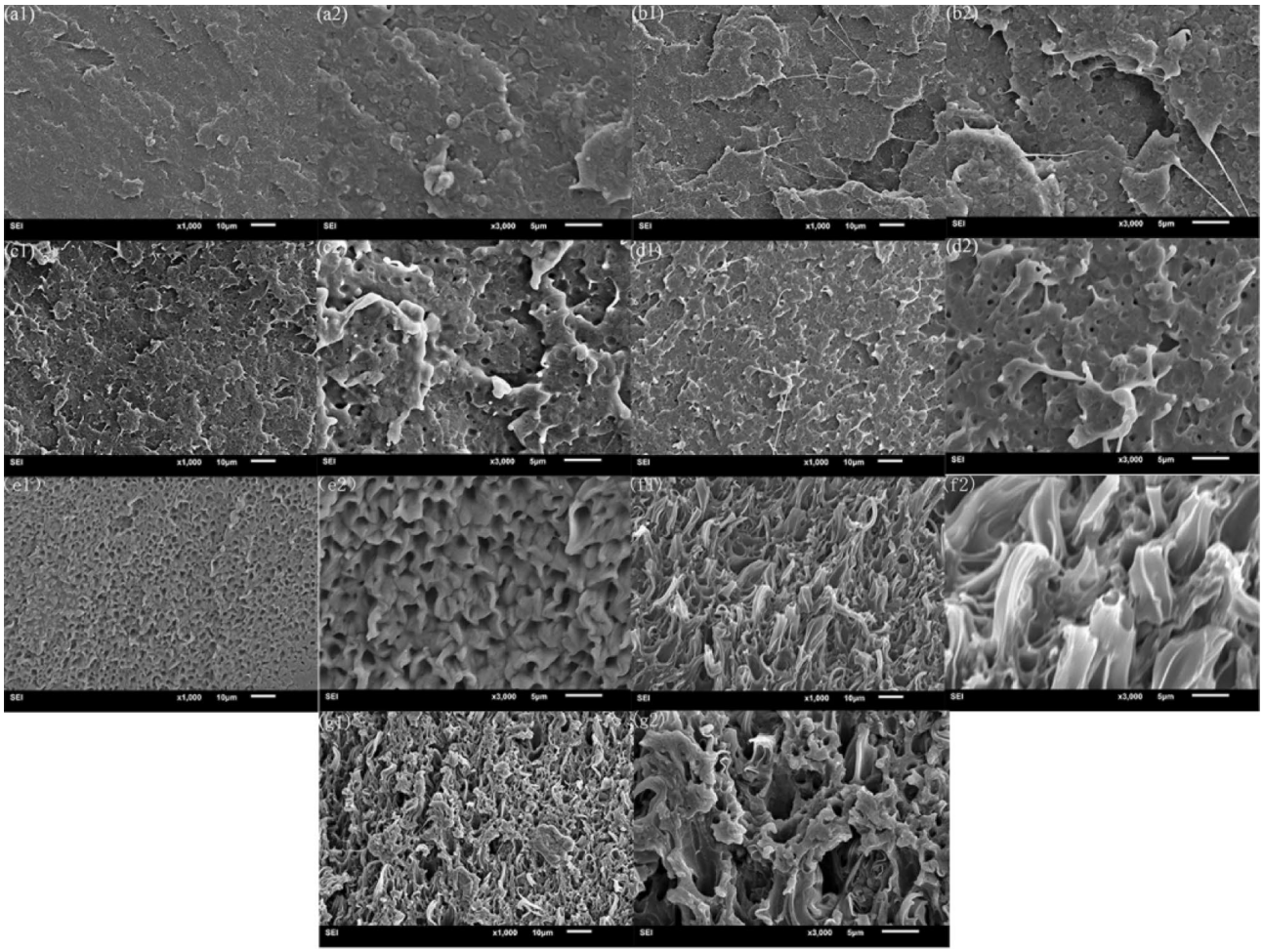

Fig. 11 SEM micrographs of fracture surface of the blends with different AXP contents from (**a**) P0-20, (**b**) P5-20, (**c**) P10-20, (**d**) P15-20, (**e**) P20-20, (**f**) P25-20, (**g**) P30-20

Morphology analysis

The SEM micrographs revealed rather brittle fracture of the PLA/PBS blend (0 phr AXP) with little amount of plastic deformation with significant smooth of the impact section as shown in Fig. 11 (3000 × and 1500 × magnification). The longer "fibrils" and cavity are the morphological representation of the fact that shear yielding has happened during the impact test, contributing to a ductile break. SEM micrographs of the impact fractured surfaces presented more evidences of ductile fractures as more and longer "fibrils" and cavity can be observed from the surfaces with the addition of AXP increased. Ductile "fibrils" are watched on the impact surfaces as shown in Fig. 11b–g. By comparison, these "fibrils" are observed barely in sample without AXP under 3000 × and 1500 × magnification. The Fig. 11b–g showed the surface of the blend at 5–30 phr AXP. There are more "fibrils" and roughness on the surface compared with the PLA/PBS blend (P0-20, 0 phr AXP). It proved that AXP is totally dispersed into blend

Fig. 12 Photograph of the samples with P30-20 after impact test

matrix, which made the blend more toughness. When the AXP addition is 30 phr, plastic deformation of the blend reached the maximum, which can explain the incomplete fracture of the blend after being impacted. Figure 12 is shown the display diagram of P30-20 spline after impact performance test. Figure 6a showed the surface of the blend at 20 wt% PBS, which is more fibrils on the surface compared with sample greater than 20 wt% PBS. It proved that the 20 wt% PBS is equally dispersed into PLA matrix, which caused the sample more toughness.

Conclusions

In this article, we focused on designing, synthesizing and applying a novel xylitol-based plasticizer to plasticize PLA/PBS blends. Evaluation of the effects of AXP as bio-based plasticizer on the mechanical property, thermal property, crystallization, rheological behavior and micromorphology of blends. It is found that the toughness of the blend is improved (the notched impact strength and elongation at break increased from 38 J/m and 39% to 527 J/m and 1286%, respectively.), with the addition of AXP increased, crystallization and processability are also enhanced. The cost of the xylitol-based plasticizer is not only lower, but also its performance matched that of commercial petro-based phthalate plasticizers, without toxic or environmental problems. It provides a new idea for the preparation of low-cost and environmentally friendly bio-based plasticizer.

References

1. Eriksen M, Mason S, Wilson S, Box C, Amato S (2013) Microplastic pollution in the surface waters of the laurentian great lakes. Mar Pollut Bull 77(s 1–2):177–182
2. Wei-Min W, Yang J, Craig, Criddle S (2017) Microplastics pollution and reduction strategies. Front Environ Sci Eng
3. Kang H, Li Y, Gong M, Guo Y, Guo Z, Fang Q et al (2018) An environmentally sustainable plasticizer toughened polylactide. RSC Adv 8(21):11643–11651
4. Qi J, Feng S, Liu X, Xing L, Xiong C (2020) Morphology, thermal properties, mechanical property and degradation of plga/ptmc composites. J Polym Res 27(12)
5. Kumar M, Mohanty S, Nayak SK, Parvaiz MR (2010) Effect of glycidyl methacrylate (gma) on the thermal, mechanical and morphological property of biodegradable pla/pbat blend and its nanocomposites. Biores Technol 101(21):8406–8415
6. Surya I, Olaiya NG, Rizal S, Zein I, Khalil H (2020) Plasticizer enhancement on the miscibility and thermomechanical properties of polylactic acid-chitin-starch composites. Polymers 12(1):115
7. Wang G, Zhang D, Li B, Wan G, Zhao G, Zhang A (2019) Strong and thermal-resistance glass fiber-reinforced polylactic acid (pla) composites enabled by heat treatment. Int J Biol Macromol
8. Nuez K, Rosales C, Perera R, Villarreal N, Pastor JM (2011) Nanocomposites of pla/pp blends based on sepiolite. Polym Bull 67(9)
9. Chuai CZ, Zhao N, Li S, Sun BX (2011) Study on pla/pbs blends. Advanced Materials Research 197–198:1149–1152
10. Al-Itry R, Lamnawar K, Maazouz A (2014) Rheological, morphological, and interfacial properties of compatibilized pla/pbat blends. Rheol Acta 53(7):501–517
11. Wang Y, Chen K, Xu C, Chen Y (2015) Supertoughened biobased poly(lactic acid)–epoxidized natural rubber thermoplastic vulcanizates: fabrication, co-continuous phase structure, interfacial in situ compatibilization, and toughening mechanism. J Phys Chem B 119(36):12138–12146
12. Massardier-Nageotte V, Benaniba M, Tahar, Maiza et al (2016) Plasticizing effects of citrate esters on properties of poly(lactic acid). J Polym Eng
13. Yang Y, Xiong Z, Zhang L, Tang Z, Zhang R, Zhu J (2016) Isosorbide dioctoate as a "green" plasticizer for poly(lactic acid). Mater Des 91:262–268
14. Takayama T, Todo M (2006) Improvement of impact fracture properties of pla/pcl polymer blend due to lti addition. J Mater Sci 41(15):4989–4992
15. Aliotta L, Vannozzi A, Canesi I, Cinelli P, Lazzeri A (2021) Poly(lactic acid) (pla)/poly(butylene succinate-co-adipate) (pbsa) compatibilized binary biobased blends: melt fluidity, morphological, thermo-mechanical and micromechanical analysis. Polymers 13(218):1–22
16. Ko SW, Hong MK, Park BJ, Gupta RK, Choi HJ, Bhattacharya SN (2009) Morphological and rheological characterization of multi-walled carbon nanotube/pla/pbat blend nanocomposites. Polym Bull 63(1):125–134
17. Park SB, Hwang SY, Moon CW, Im SS, Yoo ES (2010) Plasticizer effect of novel pbs ionomer in pla/pbs ionomer blends. Macromol Res 18(5):463–471
18. Somsunan R, Noppakoon S, Punyodom W (2019) Effect of g40 plasticizer on the properties of ternary blends of biodegradable pla/pbs/g40. J Polym Res 26(4):92
19. A, R. H., & B, N. H. A. (2013) Mechanical and thermal properties of pla/pbs co-continuous blends adding nucleating agent. Energy Procedia 34(1):871–879
20. Zhou J, Yao Z, Chang Z, Wei D, Li S (2014) Mechanical properties of pla/pbs foamed composites reinforced by organophilic montmorillonite. J Appl Polym Sci 131(18)
21. Pradeep S, Kharbas H, Turng LS, Avalos A, Lawrence J, Pilla S (2017) Investigation of thermal and thermomechanical properties of biodegradable pla/pbsa composites processed via supercritical fluid-assisted foam injection molding. Polymers 9(1):22
22. Pivsa-Art W, Fujii K, Nomura K, Aso Y, Ohara H, Yamane H (2016) The effect of poly(ethylene glycol) as plasticizer in blends of poly(lactic acid) and poly(butylene succinate). J Appl Polym Sci 133(8)
23. Elena F, Debora P, Antonio I, Andrea T, Maria KJ, Luigi T (2017) Processing conditions, thermal and mechanical responses of stretchable poly (lactic acid)/poly (butylene succinate) films. Materials 10(7):809
24. Wu S (1990) Chain structure, phase morphology, and toughness relationships in polymers and blends. Polym Eng 30(13):753–761
25. Bhatia A, Gupta RK, Bhattacharya SN, Choi HJ (2007) Compatibility of biodegradable poly (lactic acid) (pla) and poly (butylene succinate) (pbs) blends for packaging application. Korea Aust Rheol J 19(3)
26. Hao Y, Yang H, Pan H, Ran X, Zhang H (2018) The effect of mbs on the heat resistant, mechanical properties, thermal behavior and rheological properties of pla/evoh blend. J Appl Polym Sci 25(8):171
27. Wang X, Zhou J, Lin L (2007) Multiple melting behavior of poly(butylene succinate). Eur Polymer J 43(8):3163–3170

28. Ljungberg N, Wesslén B (2003) Tributyl citrate oligomers as plasticizers for poly (lactic acid): thermo-mechanical film properties and aging. Polymer 44(25):7679–7688
29. Wang H, Schultz JM, Yan S (2007) Study of the morphology of poly (butylene succinate)/poly (ethylene oxide) blends using hot-stage atomic force microscopy. Polymer 48(12):3530–3539
30. Kulinski Z, Piorkowska E, Gadzinowska K, et al (2006) Plasticization of poly (l-lactide) with poly (propylene glycol). Biomacromolecules 47(7):2128–2135
31. Rojo E, Maria Eugenia Muaoz, Anton Santamara, et al (2004) Correlation between conformational parameters and rheological properties of molten syndiotactic polypropylenes. Macromol Rapid Commun 25(14):1314–1318